Synaptic input of rat spinal lamina I projection and unidentified neurones *in vitro*

Anne Dahlhaus, Ruth Ruscheweyh and Jürgen Sandkühler

Center for Brain Research, Department of Neurophysiology, Medical University of Vienna, Vienna, Austria

Spinal lamina I projection neurones that transmit nociceptive information to the brain play a pivotal role in hyperalgesia in various animal models of inflammatory and neuropathic pain. Consistently, activity-dependent long-term potentiation can be induced at synapses between primary afferent C-fibres and lamina I projection neurones but not unidentified neurones in lamina I. The specific properties that enable projection neurones to undergo long-term potentiation and mediate hyperalgesia are not fully understood. Here, we have tested whether lamina I projection neurones differ from unidentified neurones in types or strength of primary afferent input and/or action potential-independent excitatory and inhibitory input. We used the whole-cell patch-clamp technique to record synaptic currents in projection and unidentified lamina I neurones in a transverse lumbar spinal cord slice preparation from rats between postnatal day 18 and 37. Lamina I neurones with a projection to the parabrachial area or the periaqueductal grey were identified by retrograde labelling with a fluorescent tracer. The relative contribution of NMDA receptors *versus* AMPA/kainate receptors to C-fibre-evoked excitatory postsynaptic currents of lamina I neurones significantly decreased with age between postnatal day 18 and 27, but was independent of the supraspinal projection of the neurones. We did not find a significant contribution of kainate receptors to C-fibre-evoked excitatory postsynaptic currents. Lamina I projection and unidentified neurones possessed functional $GABA_A$ and glycine receptors but received scarce action potential-independent spontaneous GABAergic and glycinergic inhibitory input as measured by miniature inhibitory postsynaptic currents. The miniature excitatory postsynaptic current frequencies were five times higher in projection than in unidentified neurones. The predominance of excitatory synaptic input to projection neurones, taken together with the previous finding that their membranes are more easily excitable than those of unidentified neurones, may facilitate the induction of synaptic long-term potentiation.

(Resubmitted 18 April 2005; accepted 29 April 2005; first published online 5 May 2005)
Corresponding author J. Sandkühler: Center for Brain Research, Department of Neurophysiology, Medical University of Vienna, Spitalgasse 4, A-1090 Vienna, Austria. Email: juergen.sandkuehler@meduniwien.ac.at

Most neurones in lamina I of the spinal dorsal horn are nociceptive (Seagrove *et al.* 2004), and lamina I is a key area for the integration of pain-related information and its transmission to the brain. The parabrachial area and the periaqueductal grey (PAG) are major targets of spinal lamina I projection neurones in the rat (Bernard *et al.* 1995). The majority of lamina I projection neurones expresses the neurokinin 1 (NK1) receptor for substance P (Ding *et al.* 1995; Todd *et al.* 2000). These neurones are required for full expression of hyperalgesia in various animal models of inflammatory and neuropathic pain (Mantyh *et al.* 1997; Nichols *et al.* 1999; Khasabov *et al.* 2002). Some forms of chronic pain can be aggravated by central sensitization; that is, an enhanced responsiveness of nociceptive neurones in the central nervous system. A cellular model of central sensitization is synaptic long-term potentiation (LTP, Sandkühler, 2000). Spino-parabrachial and spino-PAG neurones exhibit synaptic LTP after conditioning stimulation of primary afferent C-fibres (Ikeda *et al.* 2003; Sandkühler & Ikeda, 2003). Only a minority (∼5%) of the total lamina I neuronal population sends projections to the brain (Spike *et al.* 2003), so that unidentified lamina I neurones can be assumed to mostly represent intrinsic spinal neurones. Unidentified neurones did not show a synaptic LTP after conditioning stimulation of C-fibres (Ikeda *et al.* 2003; Sandkühler & Ikeda, 2003). It is presently not clear why lamina I projection neurones are prone to become sensitized. Intrinsic cellular properties such as membrane excitability

A. Dahlhaus and R. Ruscheweyh contributed equally to this work.

DOI: 10.1113/jphysiol.2005.088567

and/or network features such as type or strength of afferent input could have a decisive impact. Recently, we reported that lamina I projection neurones have intrinsic membrane properties that set them apart from unidentified lamina I neurones (Ruscheweyh *et al.* 2004). Here, we investigated both the primary afferent excitatory input and the action potential-independent inhibitory and excitatory input onto lamina I projection neurones and compared it with that of lamina I unidentified neurones.

Methods

Retrograde labelling of spino-parabrachial and spino-PAG neurones

All procedures used in this study conformed to the European Communities Council Directive (86/609/EEC) and were approved by the guidelines of the Austrian Federal Ministry for Education, Science and Culture. Young (postnatal day 18–37) Sprague-Dawley rats were anaesthetized with a mixture of ketamine and xylazine (75 mg kg^{-1} and 7.5 mg kg^{-1} I.P., respectively) and placed in a stereotaxic apparatus. A small (< 1 cm) scalp cut was made and a hole was drilled into the skull bone to allow insertion of the needle of a 500 nl Hamilton syringe into the targeted area. The animals then received a single injection of 50–100 nl fluorescent tracer (1,1′-didodecyl-3,3,3′,3′-tetramethylindocarbocyanine perchlorate ($DiIC_{12}$), 1.25–2.5%) into either the right lateral parabrachial area or the right ventrolateral and lateral PAG according to the atlas of Swanson (1992). The head wound was sewed with two stitches. Daily inspection revealed no signs of infection. After recovery from anaesthesia, the animals fed and drank normally. No pain-related behaviour was observed in any of the animals. After a 3- to 4-day survival period, preparation of spinal cord slices was carried out as described below and the rats were then killed by an overdose of ether. The brain was removed, cooled to −20°C in isopentan and cryostat sections (30 μm thick) of the brainstem were obtained in order to allow histological verification of the injection site (Fig. 1*A* and *B*). Only recordings from animals where the injection site was clearly confined to either the parabrachial area or the PAG were included in the present study.

Preparation of spinal cord slices

The lumbar spinal cord was removed under deep ether anaesthesia and the rat was killed by an overdose of ether. Transverse 500 μm thick lumbar spinal cord slices were cut on a microslicer (DTK-1000, Dosaka EM, Kyoto, Japan). In some slices a long (7–15 mm) dorsal root was preserved to allow stimulation of primary afferents. For part of the miniature inhibitory postsynaptic current (mIPSC) recordings, parasagittal slices of 400 μm thickness were made. Slices were incubated in a solution that consisted of (mM): NaCl 95, KCl 1.8, KH_2PO_4 1.2, $CaCl_2$ 0.5, $MgSO_4$ 7, $NaHCO_3$ 26, glucose 15 and sucrose 50, and was oxygenated with 95% O_2–5% CO_2; pH 7.4, osmolarity 310–320 mosmol l^{-1}. A single slice was then transferred to the recording chamber and continuously superfused with oxygenated recording solution at 3 ml min^{-1}. The recording solution was identical to the incubation solution except for (mM): NaCl 127, $CaCl_2$ 2.4, $MgSO_4$ 1.3 and sucrose 0. Experiments were conducted at room temperature (21–25°C).

Patch-clamp recording

Dorsal horn neurones were visualized with 'Dodt' infrared optics (Dodt *et al.* 1998). Retrogradely labelled lamina I projection neurones were detected by epifluorescence. They were found to lie within a distance of maximally 20 μm from the dorsal white/grey matter border (Fig. 1*Ca* and *Da*), corresponding to the zone where the tangential orientation of the neuropil typical of lamina I was observed. Randomly selected unlabelled neurons were labelled 'unidentified'. (Fig. 1*Ea*). Spino-parabrachial, spino-PAG and unidentified lamina I neurones were recorded in the whole-cell patch-clamp configuration (Fig. 1*Cb–Eb*). Patch pipettes (2–6 MΩ) from borosilicate glass (Hilgenberg, Malsfeld, Germany) were made on a horizontal micropipette puller (P-87, Sutter Instruments, Novato, CA, USA) and filled with a solution that consisted of (mM): potassium gluconate 120, KCl 20, $MgCl_2$ 2, Na_2ATP 2, NaGTP 0.5, Hepes 20 and EGTA 0.5; pH adjusted to 7.28 with KOH, measured osmolarity ∼300 mosmol l^{-1}. Neurones were recorded in current- and voltage-clamp modes using an Axopatch 200B patch-clamp amplifier and the pCLAMP 8 and 9 acquisition software (both Axon Instruments, Union City, CA, USA). Signals were low-pass filtered at 2–10 kHz, sampled at 10–100 kHz and analysed off-line using pCLAMP 8 and 9 and Mini Analysis (v.5.6.3, Synaptosoft, Inc., Decatur, USA). Membrane potentials were held at −70 mV during voltage-clamp experiments. No correction for the liquid junction potential was made. At the end of the experiments the mediolateral locations of the recorded lamina I neurones were assessed by visually inspecting the position of the pipette tip under a 4 × objective.

Passive membrane properties

Passive membrane properties were investigated as previously described (Ruscheweyh *et al.* 2004). The membrane potential measured immediately after establishing the whole-cell configuration was called the

'resting membrane potential'. Neurones with a resting membrane potential less negative than −50 mV were excluded from further investigation. The membrane capacitance was calculated from the area under the capacitive transient of the averaged reaction to 20 100 ms-long hyperpolarizing voltage steps from −70 to −80 mV.

Miniature excitatory and inhibitory postsynaptic currents

For investigation of AMPA/kainate receptor-mediated miniature excitatory postsynaptic currents (mEPSCs), voltage-clamp recordings were conducted in the presence of tetrodotoxin (TTX, 0.5 μM), D-2-amino-5-phosphonovaleric acid (D-AP5, 50 μM) (−)-bicuculline methiodide (bicuculline, 10 μM) and strychnine (4 μM). Samples of 2 to 5 min length were obtained to analyse the frequency, amplitude and the kinetics of mEPSCs in spinal lamina I neurones. Samples (4 min long) of mIPSCs were recorded in the presence of TTX (0.5 μM), D-AP5 (50 μM), 6-cyano-7-nitro-quinoxaline-2,3-dione (CNQX, 10 μM) and either strychnine (300 nM or 4 μM; for recording of GABAergic mIPSCs) or bicuculline (10 μM; for recording of glycinergic mIPSCs). Due to the ratio of intracellular to extracellular Cl^- concentrations set by our solutions, Cl^- currents (e.g. currents through $GABA_A$ and glycine receptors) are inwardly directed at a holding potential of −70 mV. Antagonists used to investigate miniature synaptic currents were added to the bath ≥ 10 min before starting the experiment. Only recordings with access resistances of less than 25 MΩ (mean 17.4 ± 0.9 MΩ, $n = 44$) that were stable throughout the entire recording (< 20% change) were considered acceptable for analysis of mPSCs. In some

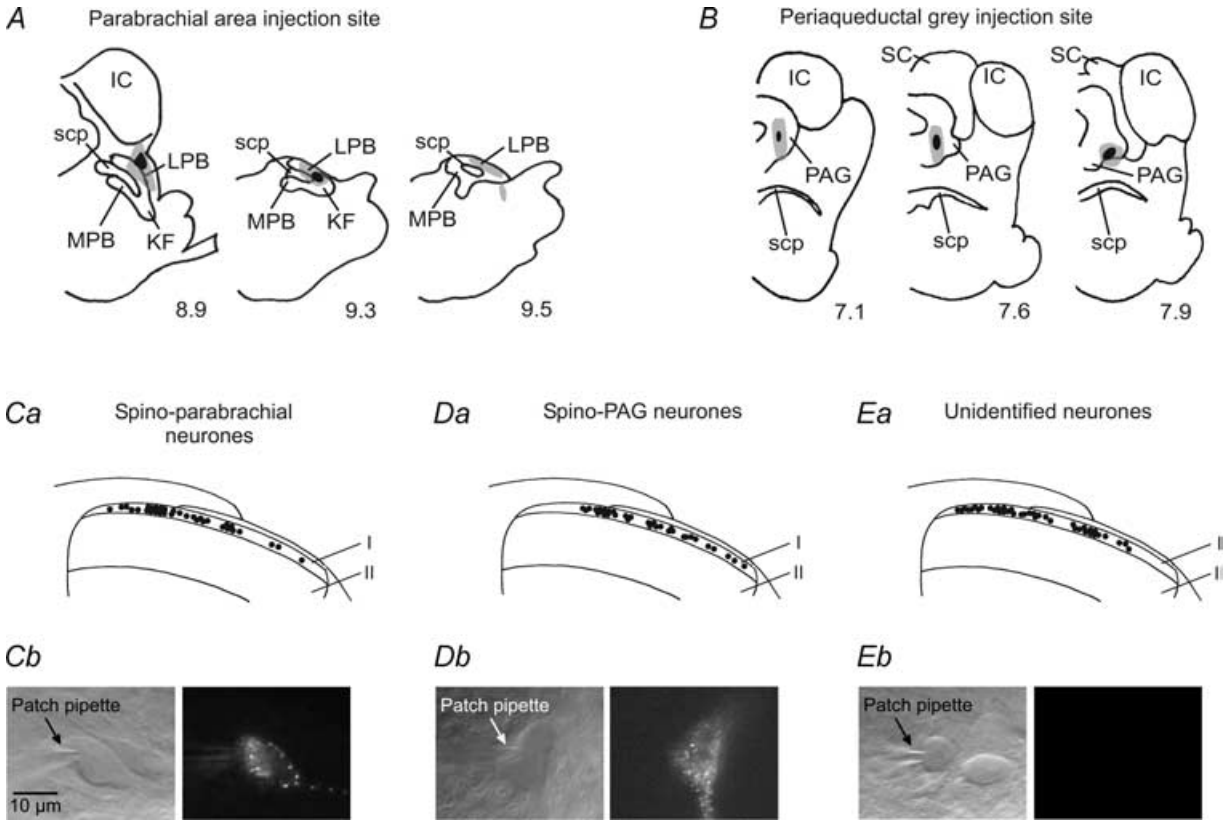

Figure 1. Retrograde labelling and recording of lamina I projection and unidentified neurones
A and *B*, the distribution of 50–100 nl DiI injected into either the right lateral parabrachial area (*A*) or the right ventrolateral and lateral PAG (*B*) in representative animals. KF, Kölliker-Fuse nucleus; LPB, lateral parabrachial area; MPB, medial parabrachial area; scp, superior cerebellar peduncle; IC, inferior colliculus; SC, superior colliculus; PAG, periaqueductal grey. Black indicates the area damaged by the injection; grey indicates the spread of the tracer. The numbers below each section indicate the distance in millimetres caudal to bregma according to the atlas of Swanson (1992). *C–E*, the locations of the recorded spino-parabrachial, spino-PAG and unidentified neurones are indicated by black dots in *Ca*, *Da* and *Ea*. All investigated neurones lay in lamina I which corresponds to the thin strip of grey matter encased by the overlying white matter and lamina II. Pictures of individual spino-parabrachial, spino-PAG and unidentified neurones in transmission and fluorescence modes are illustrated in *Cb–Eb*. The 10 μm calibration bar is valid for *Cb–Eb*.

neurones, high initial mPSC frequencies were observed that declined rapidly over the course of the first few minutes. These neurones were excluded from analysis. Detection threshold was set at 9 pA for mEPSCs and at 10 pA for mIPSCs. Each event was inspected visually and any noise that spuriously met the trigger specifications was rejected. For the analysis of mEPSC kinetics, the events were selected on the basis of the following criteria: superimposed events were discarded and only events that had stable baselines before the rise and after the end of decay were kept for analysis. The peak amplitude was calculated as the mean of the individual peak amplitudes of all events detected in an investigated neurone. For analysis of kinetics, the mEPSCs were averaged after aligning them at 50% rise time. The rise time of the resulting current was determined from 10% to 90%, the decay time from 90% to 37% of its amplitude.

Evoked excitatory postsynaptic currents

To assess both AMPA/kainate and NMDA receptor-mediated currents, evoked excitatory postsynaptic currents (eEPSCs) were investigated in a modified recording solution that was nominally free of magnesium and in most experiments was supplemented with glycine (10 μM). Data obtained in the presence and absence of glycine were pooled as no difference in the NMDA receptor-mediated currents was detected between the two groups. N-(2,6-dimethylphenylcarbamoylmethyl) triethylammonium bromide (QX-314, 5 mM) was added to the pipette solution to prevent generation of action potentials in the investigated neurone. EPSCs were evoked in labelled and non-labelled lamina I neurones by stimulating the dorsal root with supramaximal intensities (3–5 mA at 0.1 ms) in order to recruit C-fibres. Test pulses were given at 30-s intervals through a suction electrode with an isolated current stimulator (A360, World Precision Instruments, Sarasota, FL, USA). Afferent input was classified as C-fibre-evoked based on a combination of response threshold and conduction velocity (Chen & Sandkühler, 2000). C-fibre-evoked EPSCs were considered monosynaptic by the absence of failures during 10 consecutive pulses at 1 Hz and low jitter in response latencies (Fig. 2*Aa* and *Ba*; Nakatsuka *et al.* 2000). Only cells with access resistances of less than 40 MΩ and < 50% change during the experimental recording were included into the analysis of eEPSCs. Neurones were discarded when leak currents at a holding potential of −70 mV exceeded ± 60 pA.

The synaptic response was quantified by measurement of the peak amplitude and the area under the curve of the eEPSC. The average of five consecutive responses prior to drug application served as control (Fig. 2*A* and *B*). After drug application we waited for a stable baseline before five consecutive responses were averaged to assess the effect of the drug (D-AP5 and CNQX for 5–10 min, GYKI 52466 for 20 min). The NMDA receptor-mediated response was isolated for each neurone by subtraction of the averaged eEPSC curve after application of D-AP5 from the averaged eEPSC curve prior to drug application. Measurement of all areas was then taken from the onset of the NMDA receptor-mediated curve to the time point when it had declined to 10% of its peak amplitude. The NMDA receptor-mediated proportion was expressed in percentage of the total eEPSC area.

Statistical analysis

All values are expressed as mean ± S.E.M. One-way ANOVA, the non-parametric Mann-Whitney *U* rank sum test, Wilcoxon signed rank test, Student's paired and unpaired *t* test, linear regression, analysis of covariance and the Kolmogorov-Smirnov test were used for statistical comparison where appropriate. The critical value for statistical significance was set at $P < 0.05$ (*) or $P < 0.01$ (**).

Application of drugs

Drugs were applied to the perfusion solution at known concentrations. The drugs used were bicuculline (10 μM), strychnine (300 nM, 4 and 8 μM), glycine (10 μM and 1 mM), GABA (1 mM), kainate (100 μM; all from Sigma, Deisenhofen, Germany), D-AP5 (50 μM), CNQX (10 μM), TTX (0.5 and 1 μM; all from Alexis, Grünstadt, Germany), picrotoxin (100–200 μM), GYKI 52466 (100 μM) and (2*S*,4*R*)-4-methylglutamate (SYM 2081, 1–10 μM; all from Tocris, Bristol, UK). $DiIC_{12}$ (1.25–2.5%, Molecular Probes, Oregon, USA) was used as fluorescent tracer for neuronal labelling. QX-314 (5 mM, Sigma) was added to the pipette solution to investigate dorsal root-evoked EPSCs.

Stock solutions were prepared by dissolving bicuculline, glycine, GABA, kainate, D-AP5 and GYKI 52466 in distilled water, strychnine, CNQX and $DiIC_{12}$ in dimethyl sulfoxide (DMSO, Sigma), SYM 2081 in NaOH, picrotoxin in ethanol and TTX in acidic buffer (pH 4.8). Stock solutions were stored in aliquots at −20°C except for $DiIC_{12}$ which was stored at 4°C.

For exogenous application of kainate (100 μM), GABA (1 mM) and glycine (1 mM), oxygenated recording solution containing the respective drug was applied by means of a gravity-fed tube system operated by a manual switch that had its outlet opening directly onto the surface of the slice.

Results

After injection of $DiIC_{12}$ into the parabrachial area or the PAG most spinal lamina I projection neurones were found

contralateral to the injection site which is in line with previous reports (Hylden *et al.* 1989; Ruscheweyh *et al.* 2004). In the present study, we obtained whole-cell patch-clamp recordings from 148 lamina I neurones (Fig. 1*C–E*) which were either retrogradely labelled from the parabrachial area ($n = 38$) or the PAG ($n = 44$) or unidentified ($n = 66$).

Characteristics of primary afferent, monosynaptic C-fibre input to lamina I projection and unidentified neurones

Activation of different ionotropic glutamate receptors may mediate monosynaptic C-fibre-evoked EEPSCs. Here, we quantitatively evaluated the contribution of NMDA, AMPA and kainate receptor-mediated currents to the eEPSC in projection and unidentified neurones in lamina I spinal dorsal horn. In slices from Sprague-Dawley rats between 18 and 37 days old, supramaximal stimulation of dorsal roots (3–5 mA, 0.1 ms) monosynaptically evoked C-fibre responses (threshold, 0.36 ± 0.03 mA; conduction velocity, 0.32 ± 0.03 m s^{-1}; $n = 23$) in lamina I neurones which were recorded in nominally Mg^{2+}-free solution (Fig. 2*A* and *B*).

Age dependence of the eEPSC area and its NMDA and AMPA/kainate receptor-mediated portions. NMDA receptors mainly contribute to the falling phase, not the peak of the eEPSC (Forsythe & Westbrook, 1988; Yoshimura & Jessell, 1990). Consequently, we determined the area under the current (see Methods) to compare NMDA and non-NMDA receptor-mediated portions of the eEPSC. Inspection of the total eEPSC areas suggests that they decrease with increasing age of the animal (Fig. 2*C*), following a non-linear dependence. To determine what kind of non-linear dependence is adequate to describe the data, a multiple of the existing data points would have been required, which was beyond the scope of the study. Therefore, it was not possible to determine whether the groups of projection neurones and unidentified neurones were homogeneous with respect to the total eEPSC area, but the distributions of eEPSC areas clearly overlapped among these groups.

The NMDA receptor antagonist D-AP5 (50 μM) was washed into the bath to investigate the NMDA receptor-mediated proportion of eEPSCs (Fig. 2*A* and *B*). Averaged over all age groups, D-AP5 (50 μM) reduced the eEPSC area of the investigated neurones to $51 \pm 4\%$ of control (postnatal day 26 ± 1, $n = 23$; $P < 0.01$). A display of the NMDA receptor-mediated current area (Fig. 2*D*) shows a developmental current decay that at the first sight looks similar to that of the total eEPSC area (Fig. 2*C*). However, if the NMDA receptor-mediated proportion of the eEPSC area (in percent) is illustrated, it becomes clear that the NMDA receptor-mediated current area decays more strongly with increasing age than the total eEPSC area (Fig. 2*E*). Between postnatal day 18 and 27, there was a significant decrease in the NMDA receptor-mediated proportion of the eEPSC area that could be fitted by a linear function (Fig. 2*E*, $n = 18$; $P < 0.01$ for the linear dependence). The linear dependence was tested together with the homogeneity of the groups in an analysis of covariance setting. The result was that projection and unidentified neurones are homogenous with respect to the developmental changes between postnatal day 18 and 27 (the homogeneity could not be rejected with $P = 0.211$). Obviously, the linear dependence cannot hold true for age values outside the studied age range, as the NMDA receptor-mediated current proportion would become negative around postnatal day 34. The additional data points at postnatal day 35–37 suggest that a steady state is reached around postnatal day 26 (Fig. 2*E*). In line with the results of other studies (Forsythe & Westbrook, 1988; Yoshimura & Jessell, 1990), the peak amplitude of the monosynaptic eEPSC was only slightly reduced by D-AP5 (50 μM; to $87 \pm 2\%$ of control, postnatal day 26 ± 1, $n = 23$; $P < 0.01$). The NMDA receptor-mediated current was determined by subtraction of the eEPSC after application of D-AP5 from the eEPSC before D-AP5 application as described in the Methods. Where possible, the decay of the NMDA receptor-mediated current was fitted with a single exponential. The resulting decay time constant (Fig. 2*F*) decreased with increasing age of the animal.

The eEPSC current remaining after application of D-AP5 was abolished by the AMPA/kainate receptor antagonist CNQX (10 μM, $n = 7$; data not shown). Therefore, the AMPA/kainate receptor-mediated proportion of the eEPSC area exhibited an age-dependent increase from postnatal day 18–27 in projection and unidentified neurones (data not shown) reciprocal to the decrease in the NMDA receptor-mediated proportion described above.

Kainate receptor-mediated portion of the eEPSC. Recent electrophysiological studies showed that besides NMDA and AMPA receptors, postsynaptic kainate receptors in superficial dorsal horn neurones are activated following stimulation of high-threshold primary afferents, presumably C-fibres (Li *et al.* 1999). In the present study, we tested the contribution of kainate receptor-mediated currents to C-fibre-evoked EPSCs in lamina I neurones. We applied the selective non-competitive AMPA receptor antagonist GYKI 52466 (100 μM) which nearly abolished the eEPSC amplitude remaining after application of D-AP5 (reduction from $90.6 \pm 3.2\%$ to $4.4 \pm 1.1\%$ of control value before application of D-AP5, postnatal day 22.8 ± 1, $n = 11$, projection and unidentified neurones data pooled; $P < 0.01$, Figs 2*A* and *B*, and 3*Aa*). All residual currents were eliminated by CNQX (10 μM;

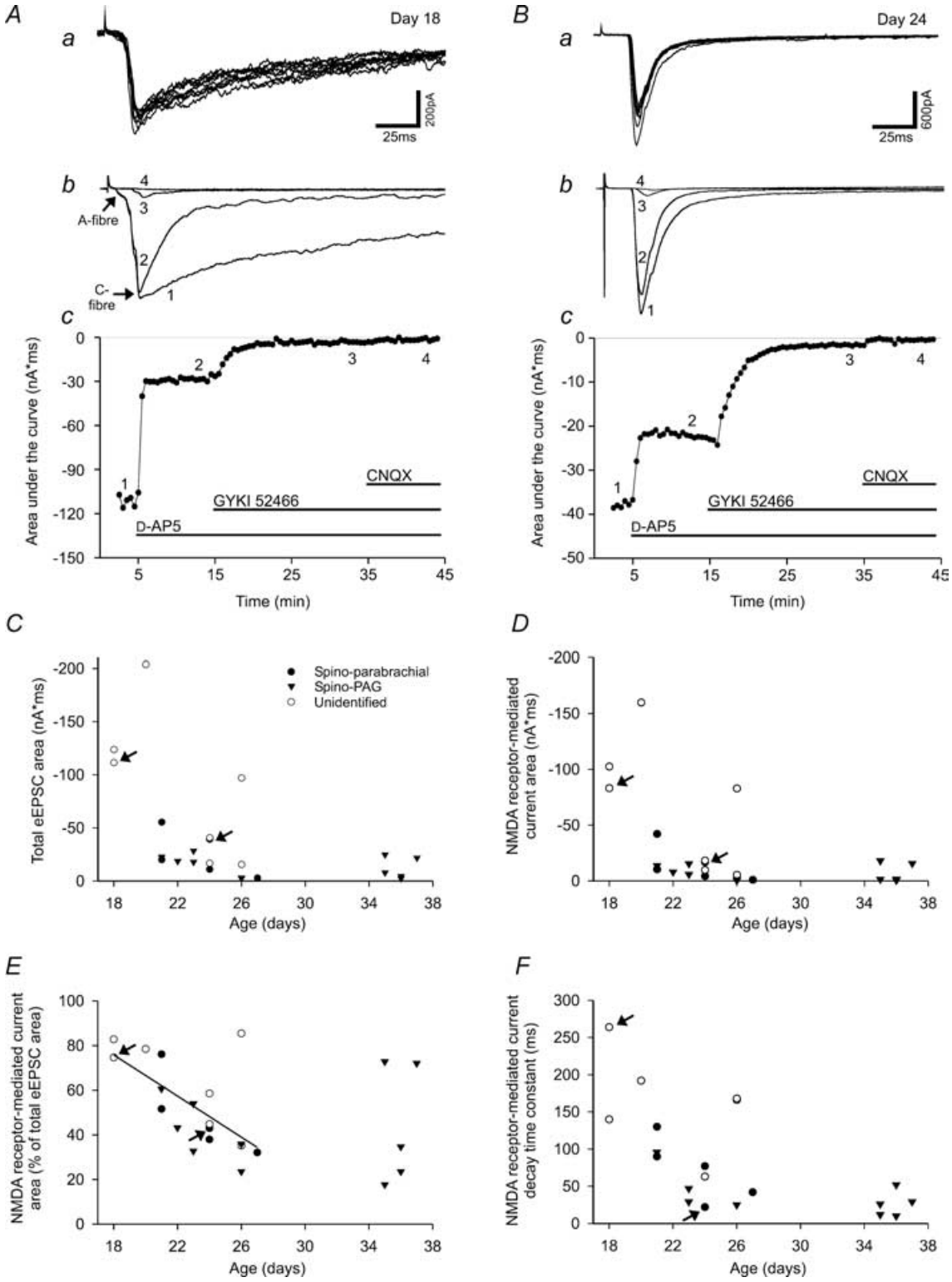

Figure 2. Developmental changes in monosynaptic C-fibre-evoked EPSCs
A and *B*, examples of monosynaptic C-fibre-evoked EPSCs at postnatal day 18 and 24. Upper traces (*a*) show the response to repetitive stimulation at 1 Hz. Absence of failures and constant latencies were taken as indication of the monosynaptic nature of the responses. The eEPSC in *A* consists of a large C-fibre-component (threshold 200 μA) and a small A-fibre-component (threshold 40 μA) as indicated in *Ab*. Latencies of the C-fibre-evoked responses and lengths of the dorsal roots were 10 ms and 4.5 mm in *A* and 15 ms and 4 mm in *B*, corresponding to conduction velocities of 0.5 m s^{-1} and 0.3 m s^{-1}, respectively. The middle traces (*b*) show the responses (each

$n = 10$, Figs 2*A* and *B*, and 3*A*). To test whether the current remaining after application of D-AP5 (50 μM) and GYKI 52466 (100 μM) was truly kainate receptor-mediated or due to incomplete blocking of AMPA receptors by GYKI 52466, we used the kainate receptor desensitizing compound SYM 2081 (1–10 μM). It reduced the eEPSC amplitude only marginally (from $7.8 \pm 4.1\%$ to $5.5 \pm 3.3\%$ of control, $n = 2$; Fig. 3*A*, traces 3 and 4) whereas, in contrast, bath application of CNQX (10 μM) eliminated the residual currents (reduction to $0.7 \pm 0.2\%$ of control, $n = 2$; Fig. 3*A*, trace 5).

Thus, we found no evidence for a major contribution of kainate receptor-mediated currents to the monosynaptic C-fibre-evoked responses. Next, we applied kainate to investigate whether functional kainate receptors were present on spinal dorsal horn lamina I neurones in rats at postnatal day 21–26. Bath application of kainate (100 μM) for 5 s to unidentified neurones in the presence of TTX (1 μM) evoked currents with an amplitude of -463 ± 53 pA ($n = 6$; Fig. 3*Ba* and *Bb*, left-hand traces). Responses did not significantly change when kainate was re-applied regardless of the absence ($94.3 \pm 4.9\%$ of control, $n = 3$; Fig. 3*Ba*, right-hand trace) or presence of SYM 2081 (10 μM; $92.7 \pm 4.1\%$ of control, $n = 3$; Fig. 3*Bb*, right-hand trace). We then repeated the experiment in the presence of TTX (1 μM) and GYKI 52466 (100 μM). Under these conditions, we observed kainate-evoked currents with an amplitude of -37 ± 11 pA ($n = 6$; Fig. 3*Ca* and *Cb*, left-hand traces). Re-application of kainate after 5 min in the absence of SYM 2081 evoked currents with amplitudes of $58.3 \pm 8.6\%$ of control ($n = 3$; Fig. 3*Ca*, right-hand trace) which were not significantly different from currents evoked in the presence of SYM 2081 (10 μM; reduction of response amplitude to $58.3 \pm 4\%$ of control, $n = 3$; Fig. 3*Cb*, right-hand trace). TTX (1 μM) and, where appropriate, GYKI 52466 (100 μM) were washed in for at least 15 min prior to application of kainate.

In conclusion, the present experiments did not reveal a major contribution of kainate receptors to responses of lamina I neurones following stimulation of primary afferent C-fibres or bath application of kainate.

Higher mEPSC frequency in lamina I projection neurones than in unidentified neurones

The action potential-independent excitatory input to projection and unidentified neurones in lamina I was investigated by mEPSC recordings in animals between postnatal day 20 and 26**.** Individual traces and averaged miniature currents are shown in Fig. 4*A*–*C*. Results are summarized in Table 1.

Projection neurones exhibited mEPSC frequencies five times higher than those of unidentified neurones ($0.86 \pm 0.11\ s^{-1}$, $n = 19$ *versus* $0.18 \pm 0.04\ s^{-1}$, $n = 10$; $P < 0.01$). Within the group of projection neurones, spino-PAG neurones showed higher mEPSC frequencies than spino-parabrachial neurones (Table 1, $P < 0.05$). Consistently, the mean inter-event interval histograms of all three groups were significantly different (Fig. 4*D*, Kolmogorov-Smirnov test followed by Bonferroni adjustment: unidentified *versus* spino-parabrachial or spino-PAG neurones, $P < 0.01$; spino-parabrachial *versus* spino-PAG neurones, $P < 0.05$). Lamina I projection neurones have been reported to have larger somata than unidentified neurones (Ruscheweyh *et al.* 2004). Because a larger neuronal surface may sustain a larger number of synapses, we calculated the mEPSC frequency of a neurone in relation to its membrane capacitance, which represents an estimate for the somatodendritic cell surface area (spino-parabrachial neurones, 77 ± 6 pF, $n = 17$; spino-PAG neurones, 71 ± 5 pF, $n = 31$; unidentified neurones, 42 ± 7 pF, $n = 10$). Membrane capacitances in the present study were measured in the presence of the various drugs used for recording mPSCs and eEPSCs and thus have to be interpreted with caution. However, the present results were very similar to those obtained previously in drug-free recording solution (Ruscheweyh *et al.* 2004). In relation to their membrane capacitance,

as an average of five consecutive traces) to dorsal root stimulation under control conditions (curve 1), in steady state after application of the NMDA receptor antagonist D-AP5 (50 μM, curve 2), the AMPA receptor antagonist GYKI 52466 (100 μM, curve 3) and the mixed AMPA/kainate receptor antagonist CNQX (10 μM, curve 4). The graphs in *Ac* and *Bc* show responses of the same neurones measured as the area under the curve *versus* time. At postnatal day 18 (*A*), the NMDA receptor-mediated proportion of the C-fibre-evoked EPSC was significantly larger than at postnatal day 24 (*B*). *C* and *D*, both the total eEPSC area and the NMDA receptor-mediated eEPSC area decrease with increasing age of the animals. *E*, between postnatal day 18 and 27, analysis of covariance revealed a significant ($P < 0.01$) linear dependence of the NMDA receptor-mediated proportion of the eEPSC on postnatal age but no influence of the type of the neurone (unidentified, spino-parabrachial or spino-PAG). The relative proportion of the NMDA current decreased from 75.8% at postnatal day 18 to 34.4% at postnatal day 27 (linear regression: $f(x) = -4.6x + 158.7$). Additional data points between postnatal day 35 and 37 show that no further decrease of NMDA receptor-mediated currents occurs after *ca* postnatal day 26–27. *F*, the decay time constant of the NMDA receptor-mediated current also decreases with increasing postnatal age. *C–F,* arrows refer to the neurones that are illustrated in *A* (postnatal day 18) and *B* (postnatal day 24). ●, spino-parabrachial neurones; ▽, spino-PAG neurones; ○, unidentified neurones.

spino-PAG neurones had mEPSC frequencies almost twice as high as those of spino-parabrachial neurones, and four times as high as those of unidentified neurones. Mean amplitudes, rise times and decay times were not significantly different for spino-parabrachial, spino-PAG and unidentified neurones (Table 1). Mean amplitude histograms are shown in Fig. 4*E* and were not significantly different between groups (Kolmogorov-Smirnov test followed by Bonferroni adjustment, $P > 0.9$ for all three comparisons).

Recently, an age-dependent increase in mEPSC frequencies was described in superficial spinal dorsal horn from postnatal day 0–10 (Baccei *et al.* 2003). We did not observe any age dependence of mEPSC frequency between postnatal day 20 and 26.

Low frequency of mIPSCs in lamina I projection and unidentified neurones

To investigate the action potential-independent inhibitory input of lamina I neurones, we recorded glycinergic and GABAergic mIPSCs in rats between postnatal day 20 and 26. Both types of mIPSCs were very scarce. In traces of 4 min duration, only zero to four out of the nine to 12 neurones investigated per group (spino-parabrachial, spino-PAG and unidentified neurones; GABAergic and glycinergic mIPSCs) showed one to 37 mIPSCs. This corresponds to GABAergic and glycinergic mIPSC frequencies between 0 and 0.15 events s^{-1} with a median of 0 events s^{-1}. Original traces are shown in Fig. 5*C*. Due to the low occurrence of

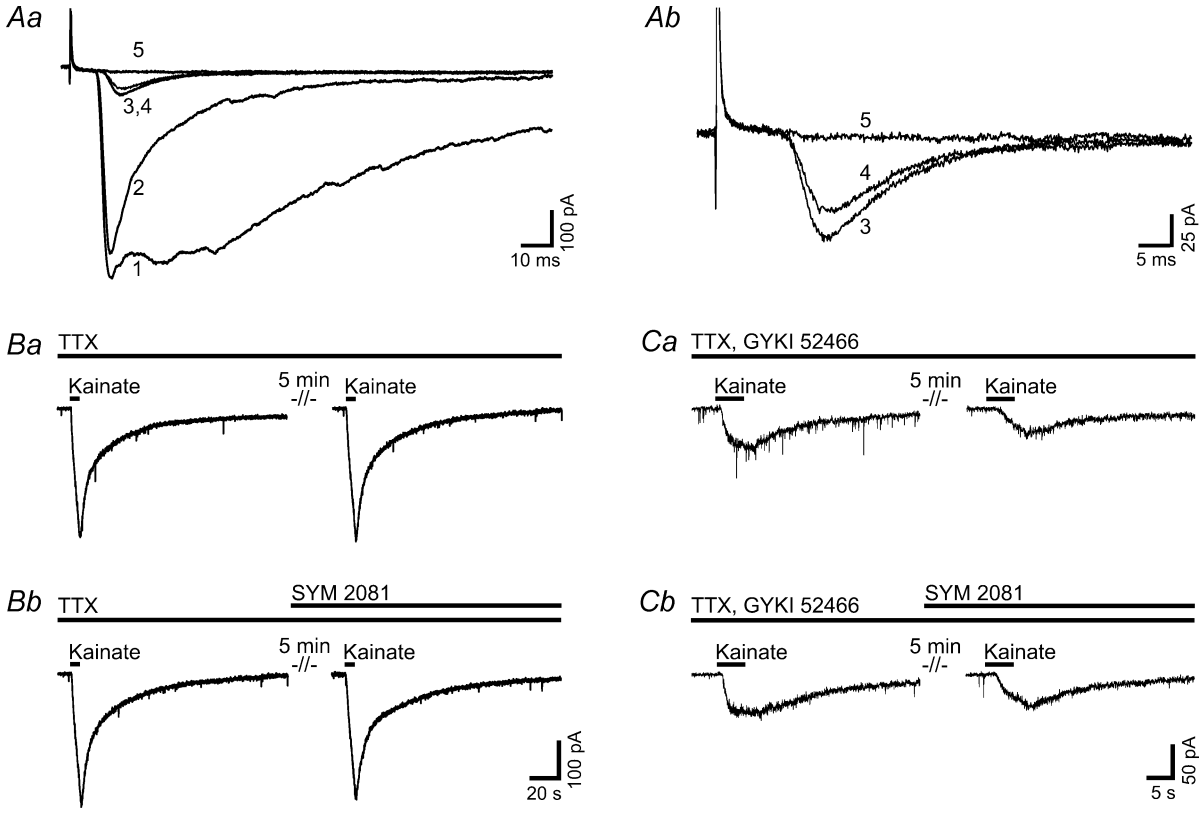

Figure 3. Kainate receptors make no major contribution to the C-fibre-evoked EPSCs of lamina I neurones between postnatal day 21 and 26

The traces illustrated in *A* are recorded from a spino-parabrachial neurone, traces in *B* and *C* from unidentified neurones. *Aa,* responses of the neurone to dorsal root stimulation (each trace represents an average of five consecutive traces) under control conditions (curve 1), in steady state after application of D-AP5 (50 μM, curve 2), the selective AMPA receptor antagonist GYKI 52466 (100 μM, curve 3), the kainate receptor desensitizing compound SYM 2081 (10 μM, curve 4) and the AMPA/kainate receptor antagonist CNQX (10 μM, curve 5). *Ab,* expanded from *Aa*. The residual current after application of GYKI 52466 (curve 3) was not abolished by SYM 2081 (curve 4) but by CNQX (curve 5). *B* and *C*, exogenous application of kainate (100 μM) for 5 s in the presence of TTX (1 μM, *B*) or TTX and GYKI 52466 (100 μM, *C*) evoked currents that could be reproduced after 5 min (*Ba, Ca*). The kainate receptor desensitizing compound SYM 2081 (10 μM) had no effect on kainate-evoked currents either in the presence of TTX (*Bb*) or in the presence of TTX and GYKI 52466 (*Cb*).

GABAergic and glycinergic mIPSCs, neither an analysis of kinetics nor a comparison between groups was attempted. The amplitudes ranged between 10.1 and 53.3 pA. These recordings were made in transversal spinal cord slices. Many lamina I neurones extend their main dendrites in rostro-caudal direction, so that transsection of major parts of the dendritic tree in the transversal slice might be a cause of the low mIPSC frequencies. Another concern was that the relatively high strychnine concentration might have partially blocked GABAergic mIPSCs (Jonas *et al.* 1998). Therefore, we conducted a series of experiments, recording GABAergic mIPSCs in the presence of a lower strychnine concentration (300 nM) in unidentified lamina I neurones of parasagittal spinal slices. Under these conditions, the mIPSC frequency was still very low (one to nine GABAergic mIPSCs in four of the eight recorded neurones) and not significantly different from the results reported above.

To elucidate whether the low mIPSC frequencies were due to the absence of $GABA_A$ and/or glycine receptors, we tested the effect of bath applied GABA (1 mM) and glycine (1 mM) on spinal lamina I neurones. The agonists were applied to the slice for 10 s in the presence of TTX (1 μM) and D-AP5 (50 μM) (both washed in for at least 10 min). All investigated neurones responded to application of both GABA and glycine with large inward currents (GABA, -687 ± 57 pA, $n = 13$; glycine, -750 ± 73 pA, $n = 13$; Fig. 5*A*) that were not significantly different between projection and unidentified neurones. No glycine-evoked currents could be recorded in the presence of strychnine (8 μM, $n = 3$) and GABA-evoked

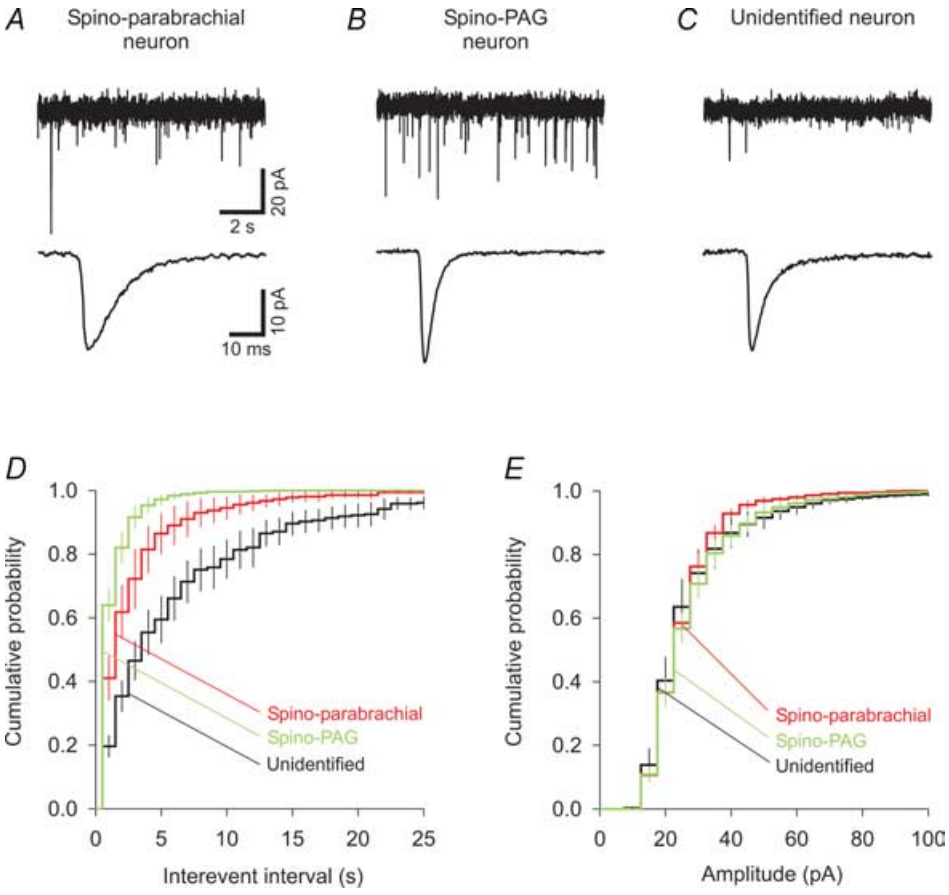

Figure 4. Mean frequencies of AMPA/kainate receptor-mediated mEPSCs differ between spino-parabrachial, spino-PAG and unidentified neurones
A–C, upper traces show representative mEPSC traces of a spino-parabrachial (*A*), a spino-PAG (*B*) and an unidentified neurone (*C*). Currents were recorded in the presence of TTX (0.5 μM), D-AP5 (50 μM), bicuculline (10 μM) and strychnine (4 μM) in voltage-clamp mode at a holding potential of -70 mV. Average mEPSCs (average of all events of the neurone, aligned at 50% rise time) are shown in the bottom traces. *D* and *E*, cumulative probability histograms illustrate the mean distribution of mEPSC inter-event intervals (bin width, 1 s) and amplitudes (bin width, 5 pA) of spino-parabrachial ($n = 9$), spino-PAG ($n = 10$) and unidentified neurones ($n = 10$). Projection neurones, especially spino-PAG neurones, exhibited shorter inter-event intervals than unidentified neurones, while amplitudes were similar.

Table 1. Properties of mEPSCs of spinal lamina I projection and unidentified neurones

	Spino-parabrachial neurones (PB) $n = 9$	Spino-PAG neurones (PAG) $n = 10$	Unidentified neurones (UN) $n = 10$
Peak amplitude (pA)	25.2 ± 1	27 ± 1.6	26.1 ± 2.4
Frequency (events s^{-1})	0.6 ± 0.13 *UN, *PAG	1.09 ± 0.14 **UN, *PB	0.18 ± 0.04 *PB, **PAG
Rise time (ms)	1.5 ± 0.2	1.2 ± 0.1	1.0 ± 0.1
Decay time (ms)	7.1 ± 0.6	5.0 ± 0.7	4.8 ± 0.6

Statistical significance was assessed by one-way ANOVA. $^{*}P < 0.05$, $^{**}P < 0.01$ in the Mann-Whitney rank sum test followed by Bonferroni adjustment. *n*, number of investigated neurones.

currents were significantly smaller in the presence of picrotoxin (100–200 μM, reduction to -53 ± 18 pA, $n = 3$; $P < 0.05$ for comparison with amplitudes obtained in the absence of picrotoxin, $n = 13$; Fig. 5*B*). Thus, the low occurrence of mIPSCs was not due to a lack of functional $GABA_A$ or glycine receptors on lamina I neurones.

Discussion

We compared the properties of several types of synaptic input of lamina I projection with those of unidentified neurones. Lamina I projection neurones displayed mEPSC frequencies five times higher than those of unidentified neurones. All lamina I neurones had very low mIPSC frequencies although they possessed functional $GABA_A$ and glycine receptors. The relative contribution of different ionotropic glutamate receptors to C-fibre-evoked EPSCs was similar for lamina I projection and unidentified neurones and underwent developmental changes between postnatal day 18 and 27.

Previous studies have revealed fundamental functional differences between lamina I projection neurones and interneurones. Projection neurones are necessary for the full expression of hyperalgesia in the rat and susceptible to LTP at their synapses with primary afferent C-fibres, while interneurones are not (Nichols *et al.* 1999; Ikeda *et al.* 2003). Retrograde labelling with DiI enabled us to record from lamina I neurones with an identified projection site in the brainstem and elucidate their differential intrinsic membrane (Ruscheweyh *et al.* 2004) and synaptic input (present study) properties. Concerning the specificity of projection areas, one has to keep in mind that many lamina I projection neurones send their axons to more than one area in the brainstem. For example, most spino-PAG neurones possess collaterals to the parabrachial area, making the spino-PAG neurones a subgroup of the spino-parabrachial neurones, accounting for about 30% of them (Spike *et al.* 2003). In addition, it has to be considered that the site of dye injection may not be identical to the final projection area of some of the studied neurones because fibres passing through the injected structures may take up the dye.

Low action potential-independent GABAergic and glycinergic inhibitory control of lamina I neurones

Exogenous application of GABA and glycine demonstrated that all investigated types of lamina I neurones expressed both functional $GABA_A$ and glycine receptors which is in line with a previous report (Chéry & De Koninck, 1999). Nonetheless, frequencies of GABA- and glycinergic mIPSCs were very low in lamina I unidentified and projection neurones. This may be due to a low spontaneous release probability of GABA and glycine and/or to a predominantly extrasynaptic location of $GABA_A$ and glycine receptors.

Evidence exists for perisynaptic and/or extrasynaptic $GABA_A$ receptors in adult rat dorsal horn (Chéry & De Koninck, 1999). Glycine receptors in cultured spinal neurones diffuse between synaptic, perisynaptic and extrasynaptic sites within seconds to minutes (Dahan *et al.* 2003). The synaptic recruitment of $GABA_A$ and glycine receptors, as well as the release probability of GABA and glycine, might be affected by different recording conditions or slice preparations (Lim *et al.* 2003) and this possibly contributes to the great variability of mIPSC frequencies in the superficial dorsal horn in the literature (0.1–5 events s^{-1}, Chéry & De Koninck, 1999; Müller *et al.* 2003). It is well established that the mIPSC frequency is not a stable feature of a spinal neurone but rather susceptible to modulation. Glycinergic and GABAergic mIPSC frequencies in spinal dorsal horn are reduced after peripheral inflammation or nerve injury (Moore *et al.* 2002; Müller *et al.* 2003) and increased by application of transmitters that may be released by descending pathways in the intact animal (noradrenaline (norepinephrine), acetylcholine; Baba *et al.* 1998; 2000*b*). It has also been reported that the frequency of $GABA_A$ receptor-mediated mIPSCs in lamina I neurones decreases with age (Keller *et al.* 2001). In the present study, mIPSC frequencies were too low to detect any age-related shift in the observation period (postnatal day 20–26).

Our finding that action potential-independent excitatory input to lamina I neurones was much more pronounced than inhibitory input could indicate that

in superficial dorsal horn either excitatory synapses outnumber inhibitory synapses or the release probability is higher for excitatory than for inhibitory transmitters. Dominance of excitatory over inhibitory action potential-independent input has also been found in lamina II neurones (Iyadomi *et al.* 2000; Wu *et al.* 2003). GABA and glycine are not the only inhibitory neurotransmitters in superficial spinal dorsal horn. Lamina I neurones may be inhibited by activation of multiple types of postsynaptic receptors, among them μ-opioid receptors, α-adrenergic receptors, cholinergic receptors and serotoninergic receptors (Aicher *et al.* 2000; Li & Zhuo, 2001).

Differences in evoked and action potential-independent excitatory synaptic input between lamina I projection and unidentified neurones

A major finding of the present study was that lamina I projection neurones exhibited significantly higher mEPSC frequencies, both absolute and in relation to their size, than unidentified neurones. Spino-PAG neurones exhibited an even higher mEPSC frequency than spino-parabrachial neurones, of which they constitute a subgroup (Spike *et al.* 2003). The most probable explanation would be that the density of excitatory synapses on the cell surface of these neurones is higher. However, the possibility cannot be excluded that projection neurones, especially spino-PAG neurones, receive synapses with a higher probability of spontaneous transmitter release. Previous recordings in the superficial dorsal horn revealed mean mEPSC frequencies between 0.14 and 12.6 events s^{-1} (Iyadomi *et al.* 2000; Baccei *et al.* 2003). We found mEPSC frequencies of 0.18 events s^{-1} in unidentified and 0.86 events s^{-1} in projection lamina I neurones. The variance between the different studies may be due to the dependence of mEPSC frequency on recording temperature (Simkus & Stricker, 2002), potassium content of the recording solution (Bao *et al.* 1998) and postnatal age of the investigated animal (Baccei *et al.* 2003). Wu *et al.* (2003), who recorded under conditions comparable to ours but from lamina II neurones, reported mean mEPSC frequencies of 1.08 events s^{-1}.

The induction of C-fibre-mediated synaptic LTP in lamina I projection neurones requires an increase in intracellular Ca^{2+} levels. The Ca^{2+} rise during conditioning repetitive stimulation is significantly stronger in lamina I projection neurones than in unidentified neurones that do not undergo LTP (Ikeda *et al.* 2003). As NMDA receptors are Ca^{2+}-permeable channels, and blockade of NMDA receptors prevents induction of LTP in projection neurones, one could suspect a difference of the NMDA receptor-mediated currents between projection and unidentified neurones. However, during the non-repetitive C-fibre stimulation which was applied here, projection and unidentified neurones had similar contributions of NMDA receptor-mediated currents to the eEPSC.

The contribution of ionotropic glutamate receptor subtypes to the C-fibre-evoked EPSC is developmentally regulated

Slice preparations from rat spinal cord are often obtained from animals which are at least 18 days old under the assumption that at this age, most of the spinal neuronal development is complete and the results obtained are therefore representative for the situation in the adult animal. However, in the present study, we describe a steep age-dependent decrease in the NMDA receptor contribution to C-fibre-evoked EPSCs in lamina I neurones between postnatal day 18 and 27. We performed

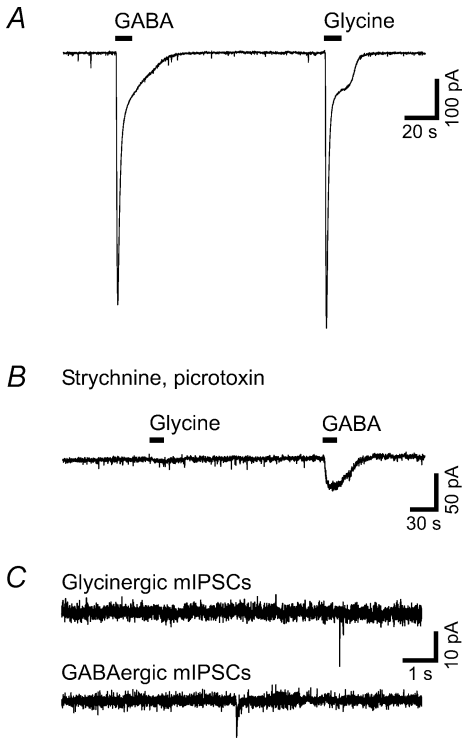

Figure 5. Lamina I neurones possess functional $GABA_A$ and glycine receptors but exhibit very low mIPSC frequencies
Results were similar for projection and unidentified neurones. The traces illustrated in *A*, *B* and the upper part of *C* are recorded from unidentified neurones; the lower trace in *C* is from a spino-PAG neurone. *A*, examples of large inward currents evoked by exogenous application of GABA (1 mM) or glycine (1 mM). *B*, the glycine-evoked inward current was blocked by strychnine (8 μM). The GABA-evoked inward current was strongly reduced by the $GABA_A$ receptor antagonist picrotoxin (200 μM). *C*, representative traces illustrate the low occurrence of glycinergic (upper trace) and GABAergic (lower trace) mIPSCs in lamina I neurones. Currents were recorded in the presence of TTX (0.5 μM), D-AP5 (50 μM), CNQX (10 μM) and either strychnine (4 μM; for recording of GABAergic mIPSCs) or bicuculline (10 μM; for recording of glycinergic mIPSCs).

our experiments in a nominally Mg^{2+}-free recording solution, to release the voltage-dependent Mg^{2+} block of the NMDA receptor (Mayer *et al.* 1984), and in the presence of glycine. Therefore, the observed developmental changes could either reflect the conversion of purely NMDA receptor-containing synapses into mixed NMDA and AMPA receptor-containing synapses or a shift in the relative proportions of AMPA receptor-mediated and NMDA receptor-mediated currents at mixed synapses. Synapses containing only NMDA receptors but no functional AMPA receptors ('silent synapses'), are present in the rat superficial dorsal horn during the first and second postnatal weeks (Li & Zhuo, 1998; Bardoni *et al.* 1998) and strongly decrease in number at later stages of development (Baba *et al.* 2000*a*). Interestingly, recent immunohistochemical results suggest that in adult rat lamina I, a relatively high number of synapses contain AMPA receptors but no NMDA receptors (Nagy *et al.* 2004).

Besides changes in the number of functional glutamate receptors, developmental modifications of the receptor properties could also account for the presently observed alterations. The developmental decrease in the decay time of NMDA receptor-mediated currents we observed points to a change in the receptor subunit composition. The results on NMDA receptor subunit distribution in spinal dorsal horn are highly controversial (see discussion in Nagy *et al.* 2004), but it has been suggested that in lamina I, the expression of the NMDA receptor subunits NR2B and NR2D decreases with postnatal age whereas subunit NR2A expression increases (Watanabe *et al.* 1994). NMDA receptors containing the NR2A subunit have significantly shorter decay times than those containing NR2B or NR2D (Monyer *et al.* 1994; Vicini *et al.* 1998), and a developmental shift towards increased NR2A expression leads to shorter decay times in rat neocortex (Flint *et al.* 1997). Similarly, the AMPA receptor subunit composition changes between postnatal day 7 and 28, accompanied by a decrease in overall AMPA receptor expression (Jakowec *et al.* 1995). Thus, the subunit composition of both NMDA and AMPA receptors undergoes developmental changes that might influence their ligand binding affinity and/or mean channel conductance and/or opening kinetics. This may lead to a shift in the relative contribution of NMDA and AMPA receptors to dorsal root-evoked EPSCs.

Kainate receptors make no major contribution to monosynaptic C-fibre-evoked responses in lamina I

It has been reported that kainate receptors are involved in primary afferent-evoked responses of superficial dorsal horn neurones at postnatal day 4–21, contributing about 30% to the combined AMPA/kainate receptor-mediated current evoked by single-shock high-intensity, presumably C-fibre, stimulation (Li *et al.* 1999). In addition, cultured dorsal horn neurones respond to exogenous application of kainate in the presence of selective AMPA receptor antagonists (Li *et al.* 1999; Kerchner *et al.* 2001). In the present study, the amplitude of the C-fibre-evoked response of lamina I projection and unidentified neurones was reduced to $< 5\%$ of control by the AMPA receptor antagonist GYKI 52466, demonstrating that if there is a kainate receptor-mediated component of the C-fibre signal, it is very small. In addition, this small residual current was resistant to the kainate receptor desensitizing compound SYM 2081 but sensitive to the mixed AMPA/kainate receptor antagonist CNQX. Equivalent results were obtained with the current evoked by exogenous kainate application. Thus, it seems most probable that the residual current was due to incomplete blocking of AMPA receptors by the AMPA receptor antagonist. At the concentration used in this study, GYKI 52466 has been reported to block about 80–90% of the AMPA receptor-mediated current. It also inhibits 20–30% of the kainate receptor-mediated current (Paternain *et al.* 1995). However, it is improbable that detection of kainate receptors was precluded by GYKI 52466, as SYM 2081 also had no effects on currents evoked by exogenous kainate application in the absence of GYKI 52466.

It can be concluded that kainate receptors make no major contribution to the C-fibre-evoked EPSC of lamina I neurones at postnatal day 21–26. Similarly, no significant contribution of kainate receptors to Aδ- or C-fibre-evoked EPSCs was found in lamina II of the adult mouse (Youn & Randić, 2004). This is consistent with the result that expression of kainate receptor subunits in spinal dorsal horn strongly decreases during development. At postnatal day 22, only moderate expression of a single subunit (KA2) is found, and it is restricted to lamina II (Stegenga & Kalb, 2001). In adult dorsal horn, expression of kainate receptors is very low compared to the expression of AMPA receptors (Tölle *et al.* 1993).

Conclusions

The present results provide further evidence for the specific role of lamina I projection neurones in the processing of nociceptive stimuli. Their prominent action potential-independent excitatory input probably has an impact on membrane excitability and discharge probability. The balance between excitation and inhibition is critical for activity-dependent plasticity and the predominance of the former may facilitate induction of synaptic LTP in projection neurones.

References

Aicher SA, Sharma S, Cheng PY, Liu-Chen L-Y & Pickel VM (2000). Dual ultrastructural localization of μ-opiate receptors and substance P in the dorsal horn. *Synapse* **36**, 12–20.

Baba H, Doubell TP, Moore KA & Woolf CJ (2000*a*). Silent NMDA receptor-mediated synapses are developmentally regulated in the dorsal horn of the rat spinal cord. *J Neurophysiol* **83**, 955–962.

Baba H, Kohno T, Okamoto M, Goldstein PA, Shimoji K & Yoshimura M (1998). Muscarinic facilitation of GABA release in substantia gelatinosa of the rat spinal dorsal horn. *J Physiol* **508**, 83–93.

Baba H, Shimoji K & Yoshimura M (2000*b*). Norepinephrine facilitates inhibitory transmission in substantia gelatinosa of adult rat spinal cord (part 1): effects on axon terminals of GABAergic and glycinergic neurons. *Anesthesiology* **92**, 473–484.

Baccei ML, Bardoni R & Fitzgerald M (2003). Development of nociceptive synaptic inputs to the neonatal rat dorsal horn: glutamate release by capsaicin and menthol. *J Physiol* **549**, 231–242.

Bao J, Li JJ & Perl ER (1998). Differences in Ca^{2+} channels governing generation of miniature and evoked excitatory synaptic currents in spinal laminae I and II. *J Neurosci* **18**, 8740–8750.

Bardoni R, Magherini PC & MacDermott AB (1998). NMDA EPSCs at glutamatergic synapses in the spinal cord dorsal horn of the postnatal rat. *J Neurosci* **18**, 6558–6567.

Bernard JF, Dallel R, Raboisson P, Villanueva L & Le Bars D (1995). Organization of the efferent projections from the spinal cervical enlargement to the parabrachial area and periaqueductal gray: a PHA-L study in the rat. *J Comp Neurol* **353**, 480–505.

Chen J & Sandkühler J (2000). Induction of homosynaptic long-term depression at spinal synapses of sensory Aδ-fibers requires activation of metabotropic glutamate receptors. *Neuroscience* **98**, 141–148.

Chéry N & De Koninck Y (1999). Junctional versus extrajunctional glycine and $GABA_A$ receptor-mediated IPSCs in identified lamina I neurons of the adult rat spinal cord. *J Neurosci* **19**, 7342–7355.

Dahan M, Lévi S, Luccardini C, Rostaing P, Riveau B & Triller A (2003). Diffusion dynamics of glycine receptors revealed by single-quantum dot tracking. *Science* **302**, 442–445.

Ding Y-Q, Takada M, Shigemoto R & Mizuno N (1995). Spinoparabrachial tract neurons showing substance P receptor-like immunoreactivity in the lumbar spinal cord of the rat. *Brain Res* **674**, 336–340.

Dodt HU, Frick A, Kampe K & Zieglgänsberger W (1998). NMDA and AMPA receptors on neocortical neurons are differentially distributed. *Eur J Neurosci* **10**, 3351–3357.

Flint AC, Maisch US, Weishaupt JH, Kriegstein AR & Monyer H (1997). NR2A subunit expression shortens NMDA receptor synaptic currents in developing neocortex. *J Neurosci* **17**, 2469–2476.

Forsythe ID & Westbrook GL (1988). Slow excitatory postsynaptic currents mediated by N-methyl-D-aspartate receptors on cultured mouse central neurones. *J Physiol* **396**, 515–533.

Hylden JL, Anton F & Nahin RL (1989). Spinal lamina I projection neurons in the rat: collateral innervation of parabrachial area and thalamus. *Neuroscience* **28**, 27–37.

Ikeda H, Heinke B, Ruscheweyh R & Sandkühler J (2003). Synaptic plasticity in spinal lamina I projection neurons that mediate hyperalgesia. *Science* **299**, 1237–1240.

Iyadomi M, Iyadomi I, Kumamoto E, Tomokuni K & Yoshimura M (2000). Presynaptic inhibition by baclofen of miniature EPSCs and IPSCs in substantia gelatinosa neurons of the adult rat spinal dorsal horn. *Pain* **85**, 385–393.

Jakowec MW, Yen L & Kalb RG (1995). *In situ* hybridization analysis of AMPA receptor subunit gene expression in the developing rat spinal cord. *Neuroscience* **67**, 909–920.

Jonas P, Bischofberger J & Sandkühler J (1998). Corelease of two fast neurotransmitters at a central synapse. *Science* **281**, 419–424.

Keller AF, Coull JAM, Chéry N, Poisbeau P & De Koninck Y (2001). Region-specific developmental specialization of GABA-glycine cosynapses in laminas I–II of the rat spinal dorsal horn. *J Neurosci* **21**, 7871–7880.

Kerchner GA, Wilding TJ, Li P, Zhuo M & Huettner JE (2001). Presynaptic kainate receptors regulate spinal sensory transmission. *J Neurosci* **21**, 59–66.

Khasabov SG, Rogers SD, Ghilardi JR, Peters CM, Mantyh PW & Simone DA (2002). Spinal neurons that possess the substance P receptor are required for the development of central sensitization. *J Neurosci* **22**, 9086–9098.

Li P, Wilding TJ, Kim SJ, Calejesan AA, Huettner JE & Zhuo M (1999). Kainate-receptor-mediated sensory synaptic transmission in mammalian spinal cord. *Nature* **397**, 161–164.

Li P & Zhuo M (1998). Silent glutamatergic synapses and nociception in mammalian spinal cord. *Nature* **393**, 695–698.

Li P & Zhuo M (2001). Cholinergic, noradrenergic, and serotonergic inhibition of fast synaptic transmission in spinal lumbar dorsal horn of rat. *Brain Res Bull* **54**, 639–647.

Lim R, Oleskevich S, Few AP, Leao RN & Walmsley B (2003). Glycinergic mIPSCs in mouse and rat brainstem auditory nuclei: modulation by ruthenium red and the role of calcium stores. *J Physiol* **546**, 691–699.

Mantyh PW, Rogers SD, Honoré P, Allen BJ, Ghilardi JR, Li J, Daughters RS, Lappi DA, Wiley RG & Simone DA (1997). Inhibition of hyperalgesia by ablation of lamina I spinal neurons expressing the substance P receptor. *Science* **278**, 275–279.

Mayer ML, Westbrook GL & Guthrie PB (1984). Voltage-dependent block by Mg^{2+} of NMDA responses in spinal cord neurones. *Nature* **309**, 261–263.

Monyer H, Burnashev N, Laurie DJ, Sakmann B & Seeburg PH (1994). Developmental and regional expression in the rat brain and functional properties of four NMDA receptors. *Neuron* **12**, 529–540.

Moore KA, Kohno T, Karchewski LA, Scholz J, Baba H & Woolf CJ (2002). Partial peripheral nerve injury promotes a selective loss of GABAergic inhibition in the superficial dorsal horn of the spinal cord. *J Neurosci* **22**, 6724–6731.

Müller F, Heinke B & Sandkühler J (2003). Reduction of glycine receptor-mediated miniature inhibitory postsynaptic currents in rat spinal lamina I neurons after peripheral inflammation. *Neuroscience* **122**, 799–805.

Nagy GG, Watanabe M, Fukaya M & Todd AJ (2004). Synaptic distribution of the NR1, NR2A and NR2B subunits of the N-methyl-D-aspartate receptor in the rat lumbar spinal cord revealed with an antigen-unmasking technique. *Eur J Neurosci* **20**, 3301–3312.

Nakatsuka T, Ataka T, Kumamoto E, Tamaki T & Yoshimura M (2000). Alteration in synaptic inputs through C-afferent fibers to substantia gelatinosa neurons of the rat spinal dorsal horn during postnatal development. *Neuroscience* **99**, 549–556.

Nichols ML, Allen BJ, Rogers SD, Ghilardi JR, Honoré P, Luger NM, Finke MP, Li J, Lappi DA, Simone DA & Mantyh PW (1999). Transmission of chronic nociception by spinal neurons expressing the substance P receptor. *Science* **286**, 1558–1561.

Paternain AV, Morales M & Lerma J (1995). Selective antagonism of AMPA receptors unmasks kainate receptor-mediated responses in hippocampal neurons. *Neuron* **14**, 185–189.

Ruscheweyh R, Ikeda H, Heinke B & Sandkühler J (2004). Distinctive membrane and discharge properties of rat spinal lamina I projection neurones *in vitro*. *J Physiol* **555**, 527–543.

Sandkühler J (2000). Learning and memory in pain pathways. *Pain* **88**, 113–118.

Sandkühler J & Ikeda H (2003). Two forms of synaptic long-term potentiation in ascending pain pathways. *2003 Abstract Viewer and Itinerary Planner*, Program No. 31.1. Washington, DC: Society for Neuroscience, 2003. Online.

Seagrove LC, Suzuki R & Dickenson AH (2004). Electrophysiological characterisations of rat lamina I dorsal horn neurones and the involvement of excitatory amino acid receptors. *Pain* **108**, 76–87.

Simkus CRL & Stricker C (2002). Properties of mEPSCs recorded in layer II neurones of rat barrel cortex. *J Physiol* **545**, 509–520.

Spike RC, Puskár Z, Andrew D & Todd AJ (2003). A quantitative and morphological study of projection neurons in lamina I of the rat lumbar spinal cord. *Eur J Neurosci* **18**, 2433–2448.

Stegenga SL & Kalb RG (2001). Developmental regulation of *N*-methyl-*D*-aspartate- and kainate-type glutamate receptor expression in the rat spinal cord. *Neuroscience* **105**, 499–507.

Swanson LW (1992). *Brain Maps: Structure of the Rat Brain*. Elsevier, Amsterdam.

Todd AJ, McGill MM & Shehab SAS (2000). Neurokinin 1 receptor expression by neurons in laminae I, III and IV of the rat spinal dorsal horn that project to the brainstem. *Eur J Neurosci* **12**, 689–700.

Tölle TR, Berthele A, Zieglgänsberger W, Seeburg PH & Wisden W (1993). The differential expression of 16 NMDA and non-NMDA receptor subunits in the rat spinal cord and in periaqueductal gray. *J Neurosci* **13**, 5009–5028.

Vicini S, Wang JF, Li JH, Zhu WJ, Wang YH, Luo JH, Wolfe BB & Grayson DR (1998). Functional and pharmacological differences between recombinant N-methyl-D-aspartate receptors. *J Neurophysiol* **79**, 555–566.

Watanabe M, Mishina M & Inoue Y (1994). Distinct spatiotemporal distributions of the N-methyl-D-aspartate receptor channel subunit mRNAs in the mouse cervical cord. *J Comp Neurol* **345**, 314–319.

Wu S-Y, Ohtubo Y, Brailoiu GC & Dun NJ (2003). Effects of endomorphin on substantia gelatinosa neurons in rat spinal cord slices. *Br J Pharmacol* **140**, 1088–1096.

Yoshimura M & Jessell T (1990). Amino acid-mediated EPSPs at primary afferent synapses with substantia gelatinosa neurones in the rat spinal cord. *J Physiol* **430**, 315–335.

Youn D-H & Randić M (2004). Modulation of excitatory synaptic transmission in the spinal substantia gelatinosa of mice deficient in the kainate receptor GluR5 and/or GluR6 subunit. *J Physiol* **555**, 683–698.

Acknowledgements

The authors wish to thank R. Dahlhaus for assistance with statistical analysis. This work was supported by the Austrian Science Fund (FWF-P15542) and the Anniversary Fund of the Österreichischen Nationalbank (ÖNB-10494). A.D. was partially supported by the Boehringer Ingelheim Fonds.